USAGE OF FRICTION-DAMPED BRACED FRAMES FOR SEISMIC VIBRATION CONTROL

An Honors Fellow Thesis

by

BRYNNAN ELYSE FINK

Submitted to Honors and Undergraduate Research
Texas A&M University
in partial fulfillment of the requirements for the designation as

HONORS UNDERGRADUATE RESEARCH FELLOW

May 2012

Major: Civil Engineering

USAGE OF FRICTION-DAMPED BRACED FRAMES FOR SEISMIC VIBRATION CONTROL

An Honors Fellow Thesis

by

BRYNNAN ELYSE FINK

Submitted to Honors and Undergraduate Research
Texas A&M University
in partial fulfillment of the requirements for the designation as

HONORS UNDERGRADUATE RESEARCH FELLOW

Approved by:

Research Advisor: Gary T. Fry
Associate Director, Honors and Undergraduate Research: Duncan MacKenzie

May 2012

Major: Civil Engineering

ABSTRACT

Usage of Friction-damped Braced Frames for Seismic Vibration Control. (May 2012)

Brynnan Elyse Fink
Department of Civil Engineering
Texas A&M University

Research Advisor: Dr. Gary T. Fry
Department of Civil Engineering

This study presents the results of experimental work that examines the functionality of friction-damped braced frames during seismic events. The simplicity and efficacy of this friction device as a means of passive vibration control suggest that it may have notable implications in the field of structural engineering. Little scholarship has been devoted to this issue in recent years, and further research to advance our understanding of its possible implementations is necessary. To measure the functionality of this type of frame, this study first examines and compares virtual models of a building modeling the effect of friction damping versus that same building without such damping. It then corroborates these findings by presenting the results of physical experimentation on a scale model of the building, both with and without damping. The validation of the virtual models by the physical model provides credence to the usage of friction-damped braced frames as a seismic energy dissipating system.

DEDICATION

This thesis is in dedication to my teacher and mother, Janna Pentecost Fink. She educated me at home through the entirety of my pre-collegiate experience and prepared me for both the challenges and successes to come. Most importantly, she provided the emotional support necessary to bolster me through the peaks and troughs of life, both within the academic realm and without. The completion of this thesis would have been impossible without her unconditional love and encouragement.

ACKNOWLEDGMENTS

I would like to acknowledge the constant encouragement and guidance of my advisor, Dr. Gary T. Fry. I would also like to express thanks to Luis Eduardo Peternell Altamira and Dr. Brett Story for the knowledge and counsel they have given and for the assistance they have provided toward the completion of this project. I am also grateful to the Center for Railway Research (CRR) research group for being an attentive audience of my presentations and for the thoughtful questions posed and advice offered over the course of the past year.

Additional gratitude is extended to my family and friends, without whose support and friendship this task would have proven to be significantly more challenging. Among the friends who were the most influential are Nathan Favero and Talya Lazerus, whose camaraderie as members of the Honors Undergraduate Research Fellows class of 2012 was treasured over the course of the past year.

NOMENCLATURE

A	Cross-sectional area
C	Constant of integration
c	Damping coefficient
Δ	Axial deformation
δ	Vertical deflection
E	Modulus of elasticity
F	Friction force
FDBF	Friction-damped braced frame
H	Horizontal applied load
h	Height
I	Second moment of area, or moment of inertia
k	Axial stiffness coefficient
L	Length
LSB joint	Limited slip bolted joint
M	Bending moment
μ	Coefficient of friction
N	Normal force
θ	Angle of rotation
P	Internal force
ρ	Radius of curvature

PED	Passive energy dissipation
SDOF	Single degree of freedom
V	Shear force
w	Transverse loading

TABLE OF CONTENTS

Page

LIST OF FIGURES

FIGURE Page

LIST OF TABLES

CHAPTER I

INTRODUCTION

During a seismic event, structures are exposed to vibrations that can cause extensive damage and threaten their structural integrity. The energy input into the building must be dissipated, and the way in which this is accomplished determines the amount of damage that is done. If the energy is consumed through bending, cracking, or twisting beyond the structural capacity of a member, permanent (or plastic) deformation can occur (Pall and Pall 2004). The repair costs in such a situation can be significant with regard to both finances and time the structure remains out of commission.

Not only is prevention of structural collapse important, but ensuring the safety of a building's contents and inhabitants is of upmost concern. Especially in the event of a severe seismic incident, facilities central to catastrophe mitigation and public health must remain in working order. The ability to gain access to hospitals and the medical equipment they contain, emergency response workers, and telecommunication, etc., is vital.

Figure 1 captures a scene following the 1995 Kōbe Earthquake in Japan, which was registered as a magnitude 7.3 on the Richter scale. The event lasted only 20 seconds, yet

---

This thesis follows the style of the *Journal of Structural Engineering*.

it caused 4,571 fatalities, with more than 14,000 injured (Encyclopædia Britannica Inc. 2012). In the foreground of Figure 1, some of the more than 120,000 damaged structures are visible. Over the course of the earthquake, the physical damage caused to these structures compromised the lives and livelihoods of many of the Kōbe citizens, contributing to the resulting devastation. In the background (Fig. 1), some structures remain erect; however, substantial reconstruction was required before the buildings were able to resume their original functionalities.

Fig. 1. Damage due to the 1995 Kōbe Earthquake in Japan (Gamesby 2012)

As the world's population continues to expand and nations continue to develop, the damage left behind by these events remains a devastating reality. Earthquakes have

resulted in thousands of deaths and have destroyed the homes and livelihoods of thousands more over the last three decades alone (Villaverde 2009). Furthermore, such disasters often significantly impact economic activity in the countries affected (Elnashai and Di Sarno 2008). Incorporating devices to control the motion induced by seismic vibrations is crucial to reducing the structural, social, and financial damage caused by earthquakes.

CHAPTER II

BACKGROUND

Numerous devices have been developed for seismic vibration control. These devices can be categorized as active, passive, or hybrid. In a conventional structure (with no added devices), a structure undergoes an excitation and produces a response (Fig. 2(a)). If a passive energy dissipater is introduced, the structure reacts similarly to a conventional structure; however, the device absorbs a portion of the seismic energy input, reducing the magnitude of the vibrations experienced by the structure (Fig. 2(b)).

Active control is slightly more complicated. Active devices (Fig. 2(c)) incorporate real-time feedback from actuators and other instrumentation installed both within the structure and on the ground to oppose the motion induced by the earthquake. As excitation occurs, sensors send a signal to a controller which activates actuators within the structure to counteract the motion of the earthquake. Motion is inevitably induced, and sensors on the structure send information about the structural response to the controller, which additionally influences the actuators. Hybrid devices (Fig. 2(d)) encompass systems exhibiting features of both the active and passive control devices (Hu et al. 1996).

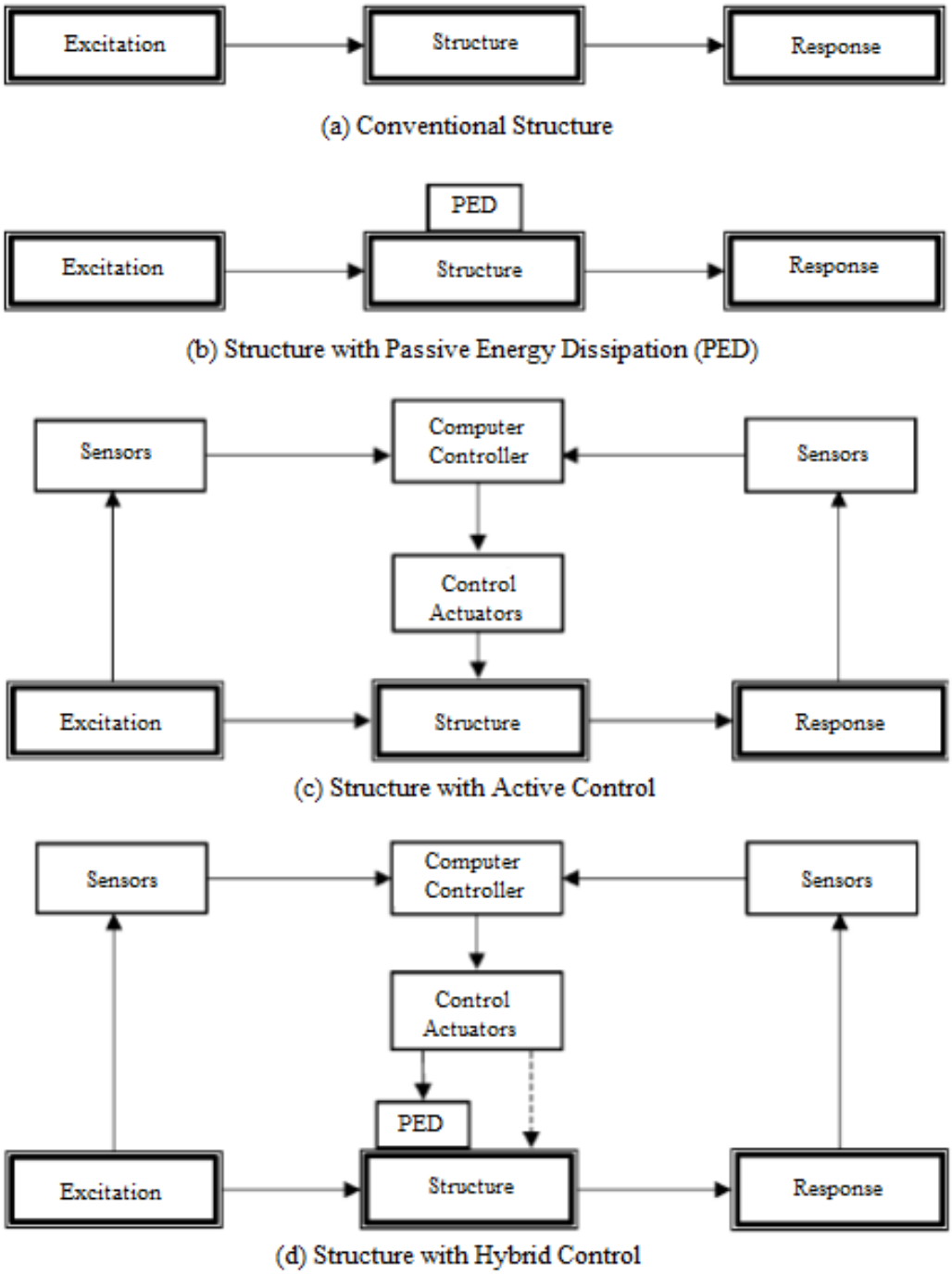

Fig. 2. Structure with various control schemes (Soong and Spencer 2002)

One of the advantages of passive energy dissipaters is that there is no potential for magnification of an earthquake's effect. In the worst plausible situation, a structure with a PED installed would react no differently during a seismic event than would a conventional structure with no device installed. However, with active and hybrid systems, there is potential for complication. In a system functioning correctly, the motion induced by the actuators will counteract the motion of the earthquake. However, if the system begins to malfunction, it is possible for the actuators to induce motion that actually supplements that induced by the earthquake, resulting in larger vibrations, larger displacements, and more damage than would occur in a conventional structure experiencing an identical seismic excitation.

Passive friction devices have a number of other advantages. As they absorb the seismic energy, the amplitude of the displacements and accelerations of the structure are reduced. Consequently, the elasticity of the structure remains intact with little to no plastic deformation. This aids in maintaining the structural integrity (Pall and Marsh 1982). Additionally, passive devices enable adjustment of the structure for an optimal response without the implementation of costly electronic devices or a complete structural redesign (Peternell 2009).

Passive vibration control methods can be divided into four categories, as described by Mead (1998):

- Vibration control by structural design

- Vibration control by localized additions
- Vibration control by resilient isolation
- Vibration control by added damping

Vibration control by structural design is only applicable if significant vibration is anticipated at the time of design. Vibration control by localized additions can be achieved through the addition of mass to adjust the natural resonance frequency of a structure or through the introduction of a vibration neutralizer, which acts to counteract the exciting force of a structure along a narrow range of frequencies. When one part of a system vibrates due to vibrations transmitted by another part through several connection points, vibration control by resilient isolation introduces a soft, or resilient, "padding" to the connection points to mitigate the transferred vibrations. Lastly, vibration control by added damping resists motion with a friction force acting opposite to the direction of movement (Mead 1998). These various methods of achieving vibration control can be implemented either alone or in combination.

As a means of seismic retrofitting, vibration control by added damping is perhaps the simplest and most cost-effective of the four aforementioned categories of passive vibration control (Pall and Pall 2004). The friction force opposes motion with a magnitude F according to equation (1).

$$F = \mu N \tag{1}$$

N is the force acting normal to the two frictional surfaces and μ is the coefficient of friction which is assumed to be independent of the relative velocities of the two surfaces

and is thus the same in both static and dynamic loading cases. Because the introduction of additional damping affects the structure's stiffness and inherent damping, the structure is able to partially dissipate the flood of seismic energy without requiring external forces or control to be applied (Mead 1998).

While the usage of friction for vibration damping has been used for decades in the automotive, military, and aerospace industries, passive friction devices as a means of seismic energy dissipation have merely an approximate 35 years of history within the structural realm (see Soong and Dargush 1997; Soong and Constantinou 1994; Keightley 1977; Keightley 1979; Soong and Constantinou 1994; Peternell 2009).

Pall, Marsh, and Fazio (1980) developed the Limited Slip Bolted (LSB) joint (Fig. 3), a connection which consists of steel plates or sections with slotted holes connected by high strength bolts to steel inserts anchored in the concrete panels. The joints are designed not to slip under normal loads (e.g. wind loads or service loads), but are expected to slip during severe seismic excitations.

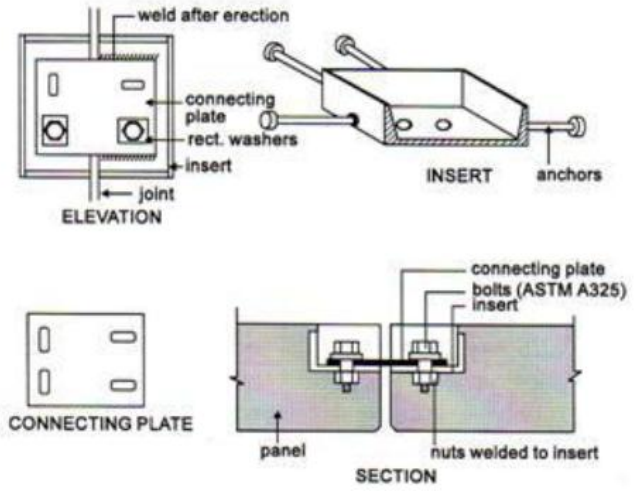

Fig. 3. Typical details of a simple wall-to-wall Limited Slip Bolted (LSB) joint (Pall et al. 1980)

The research completed regarding the LSB joint revealed a number of points of particular importance. Pall et al. (1980) listed eight distinct conclusions given the implementation of such a friction damper, the final six which are of particular relevance to this study:

> "3. The building is softened without losing its elasticity and resilience and recovers with little or no permanent set.
>
> "4. The joints act as structural dampers to control the amplitude, and as safety valves to limit the load exerted.
>
> "5. The amplitude of vibrations and accelerations are considerably reduced, hence secondary and architectural damage is minimized.
>
> "6. The building can be 'tuned' for optimum response without resorting to other expensive devices like hydraulic systems or added masses; this 'tuning' represents

matching the slip load to the anticipated maximum earthquake intensity to give minimum acceleration in the building.

"7. There is no yielding of materials involved in the process of energy dissipation, hence no damage is caused.

"8. The joints lose little or no tension, and remain without adjustment ready to face the next earthquake with the same efficiency."

The concept of energy dissipation through slipping joints demonstrated with the LSB joint can be easily extended to framed buildings. Thus Pall dampers were designed to satisfy needs in this sector. Pall dampers consist of series of steel plates, which are specially treated to develop very reliable friction. These plates are then clamped together and allowed to slip at a predetermined load (Pall and Pall 2004).

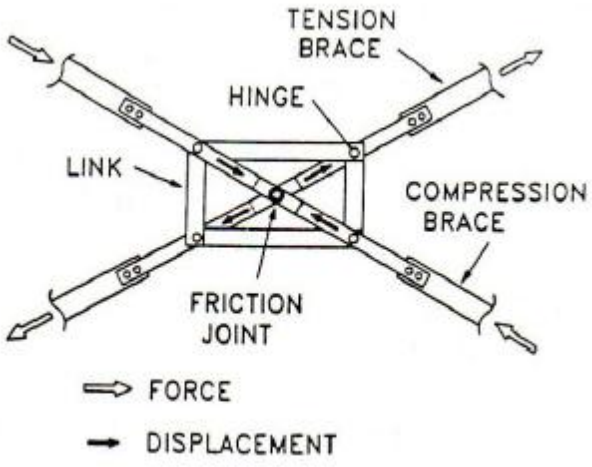

Fig. 4. Typical Pall friction damper for use with cross braces (Pall and Marsh 1982)

When a seismic excitation causes slippage within the tension brace of the Pall friction damper designed for usage with cross-bracing (Fig. 4), the device causes the other brace to go into compression, preventing buckling. Energy is dissipated in both braces through the shortening and lengthening of each brace and is simultaneously reset to counteract the next half-cycle of motion (Pall and Pall 2004; Peternell 2009).

Other models of the Pall friction damper are the single tension/compression brace (Fig. 5) and the chevron brace (Fig. 6). Due to the variety and ability to customize, Pall friction dampers are among the most successful and accepted devices in use today (Pall and Pall 2004).

Fig. 5. Single tension/compression-braced friction damper (Pall and Pall 2004)

Fig. 6. Chevron-braced friction damper (Pall and Pall 2004)

CHAPTER III

RESEARCH OBJECTIVE

Over the course of the past decade, active friction damping has been the focus of much examination. Therefore, during this time, research on passive friction damping has slowed despite its clearly evident benefits, impeding further innovation within the field. Therefore much of the prior study regarding passive friction damping has become out of date in the context of current building codes and design philosophies (Peternell 2009).

Given the readily apparent advantages of passive friction damping and the insufficiency of current research, Peternell designed a study "of around 7,000 structural analyses that [were] used to show the excellent seismic performance and economic advantages of Friction Damped Braced Frames … [and] to improve our understanding on [sic] their dynamic behavior" (Peternell 2009). Peternell's research presents thorough analytical evidence of the exceptional performance of passive friction damping; however, no experimental work has been done to support these findings.

This study will investigate the performance of passive friction damping as employed in friction-damped braced frames (FDBFs). To measure the functionality of this type of frame, this study first examines and compares virtual models of a building modeling the effect of friction damping versus that same building without such damping. It then attempts to corroborate these findings by performing physical experimentation on a scale

model of the building, both with and without damping. The author hypothesizes that the frame with friction damping will experience smaller accelerations at the first floor than will the frame without friction damping. Additionally, it is expected that experimental results will verify the results obtained by the analytical investigation, and that structural collapse will be prevented in all cases studied.

CHAPTER IV

LINEAR BEHAVIOR OF FRAMES

A method of analysis of frames involves determining the equivalent stiffness of the frame, then using Hooke's Law to find the deflection of the frame as a function of this stiffness and the applied load. This method can be applied to both moment-resisting frames and braced frames. However, due to the variation in how the loads are resisted by these two frames, the equivalent stiffnesses of each system vary as well.

Moment-resisting frames

Deflection equation

To facilitate the determination of the stiffness of a moment-resisting frame, an equation for the deflection of a beam as a function of the location along the beam is necessary. Consider the following beam (Fig. 7), with *x* measured from left to right along the axis of the beam:

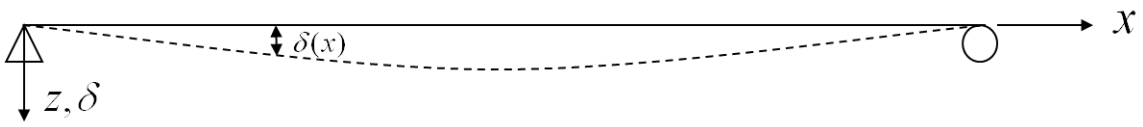

Fig. 7. Beam used in deflection derivation

From the definition of curvature *k*,

$$k(x) = \frac{1}{\rho(x)} = \frac{-\delta^{ii}(x)}{\{1+[\delta^{i}(x)]^2\}^{3/2}} = \frac{M}{EI} \tag{2}$$

where ρ is the radius of curvature, δ is the deflection of the beam, M is the bending moment, E is the modulus of elasticity, and I is the second moment of area. For small deflections δ resulting in small angles δ^i compared to unity,

$$[\delta^{i}(x)]^2 \approx 0 \quad \Rightarrow \quad \delta^{ii}(x) \approx -\frac{M}{EI}$$

Given the following relationships between the loading *w*, the shear *V*, and the bending moment *M* of a beam,

$$\frac{dV}{dx} = -w(x)$$

$$\frac{dM}{dx} = V_x$$

we can differentiate equation (2) with respect to *x* to achieve the following expressions:

$$\begin{aligned} \delta^{ii}(x) &= -\frac{M}{EI} \\ \delta^{iii}(x) &= -\frac{V_x}{EI} \\ \delta^{iv}(x) &= \frac{w(x)}{EI} \end{aligned} \tag{3}$$

Suppose $w(x) = w_o$. Integrate equation (3) four times to find an equation for $\delta(x)$.

$$\delta^{iv}(x) = \frac{w_o}{EI}$$
$$\delta^{iii}(x) = \frac{w_o x}{EI} + C_1$$
$$\delta^{ii}(x) = \frac{w_o x^2}{2EI} + C_1 x + C_2$$
$$\delta^{i}(x) = \frac{w_o x^3}{6EI} + \frac{C_1 x^2}{2} + C_2 x + C_3$$
$$\delta(x) = \frac{w_o x^4}{24EI} + \frac{C_1 x^3}{6} + \frac{C_2 x^2}{2} + C_3 x + C_4 \qquad (4)$$

To determine the constants of integration C_1 through C_4, the following initial conditions must be defined:

$$\delta(0) = \delta_o$$
$$\delta^{i}(0) = \theta_o$$
$$\delta^{ii}(0) = -\frac{M_o}{EI}$$
$$\delta^{iii}(0) = -\frac{V_o}{EI}$$

Since each term in the integrated equations (except the constants of integration) has an x in it, the constants of integration are equal to the initial conditions for each equation.

$$\delta(0) = \delta_o = C_4$$
$$\delta^{i}(0) = \theta_o = C_3$$
$$\delta^{ii}(0) = -\frac{M_o}{EI} = C_2$$
$$\delta^{iii}(0) = -\frac{V_o}{EI} = C_1$$

Substituting the values for the constants of integration back into equation (4) yields an equation for the deflection of the beam with respect to *x*.

$$\delta(x) = \delta_o + \theta_o x - \frac{M_o x^2}{2EI} - \frac{V_o x^3}{6EI} + \frac{w_o x^4}{24EI} \tag{5}$$

Equivalent stiffness

Consider the one-story, one-bay portal frame loaded as shown:

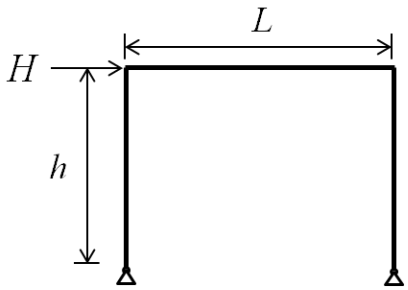

Fig. 8. Moment-resisting (portal) frame

A static analysis of the frame (Fig. 8) shows that the girder is subjected to the following internal forces (Fig. 9):

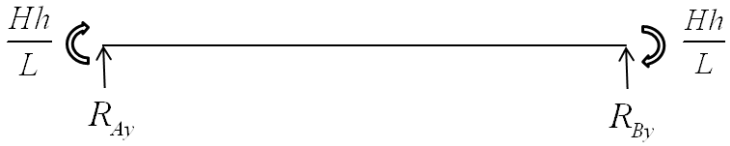

Fig. 9. Girder of moment-resisting (portal) frame and internal forces

The deflection of the girder with respect to *x* can be modeled with equation (5) by using appropriate initial values.

$$\left.\begin{aligned} \delta_o &= 0 \\ \theta_o &= ? \\ M_o &= \frac{Hh}{2} \\ V_o &= -\frac{Hh}{2} \end{aligned}\right\} \quad \delta(x) = \theta_o x - \frac{Hhx^2}{4EI} + \frac{Hhx^3}{6EIL} \tag{6}$$

When $\delta(L) = 0$ is substituted into equation (6),

$$\theta_o = \frac{HhL}{12EI} \tag{7}$$

Assuming that the columns are rigid, the frame deflection Δ_G due to the flexibility of the girder can be found. θ_o is defined as the angle through which the column rotates to achieve the frame deflection Δ_G, as shown in Figure 10.

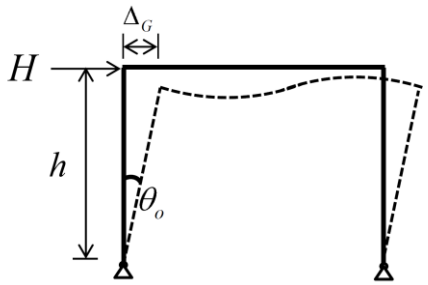

Fig. 10. Deflection of moment-resisting (portal) frame due only to girder flexibility

From the geometry of the frame,

$$\sin(\theta_o) = \frac{\Delta_G}{h}$$

$$\Delta_G = h\sin(\theta_o)$$

For small deflections θ_o,

$$\sin(\theta_o) \approx \theta_o$$

$$\Delta_G = h\theta_o \tag{8}$$

Combining equations (7) and (8) yields an equation for the frame deflection Δ_G due solely to the flexibility of the girder.

$$\Delta_G = h\frac{HhL}{12EI} = \frac{Hh^2L}{12EI}$$

Treating the girder as a spring, Hooke's Law can be used to determine the girder stiffness k_G.

$$F = k\Delta_x$$

$$H = \frac{12(EI)_G}{h^2L}\Delta_G$$

$$\therefore k_G = \frac{12(EI)_G}{h^2L}$$

Through a similar process, the stiffness k_C of each column can also be found.

$$k_C = \frac{3(EI)_C}{h^3}$$

The moment-resisting frame can be modeled as an equivalent spring system, as shown in Figure 11.

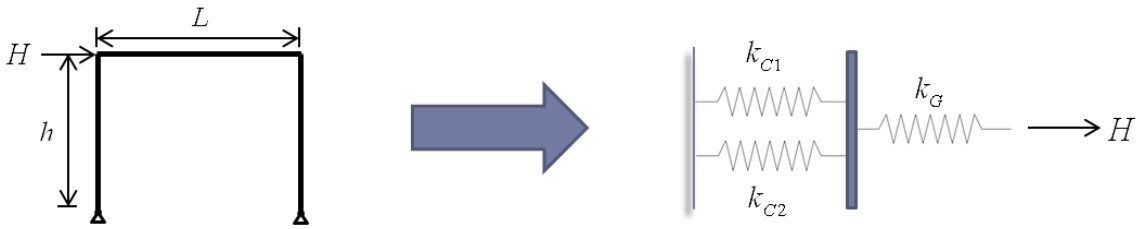

Fig. 11. Equivalent spring system for a moment-resisting (portal) frame

The columns in this system are in parallel with one another, so their equivalent stiffness $k_{eq,C}$ can be obtained by adding their individual stiffness values.

$$k_{C1} = k_{C2} = \frac{3(EI)_C}{h^3}$$

$$k_{eq,C} = k_{C1} + k_{C2} = \frac{6(EI)_C}{h^3}$$

The girder is in series with the columns, so the system's equivalent stiffness k_{eq} can be found as follows:

$$k_G = \frac{12(EI)_G}{h^2 L}$$

$$k_{eq} = \frac{k_{eq,C} k_G}{k_{eq,C} + k_G} = \frac{\frac{6(EI)_C}{h^3}\frac{12(EI)_G}{h^2 L}}{\frac{6(EI)_C}{h^3} + \frac{12(EI)_G}{h^2 L}}$$

$$k_{eq} = \frac{12(EI)_C (EI)_G}{h^2 L(EI)_C + 2h^3 (EI)_G} \tag{9}$$

The result shown in equation (9) can be further corroborated by modeling the frame (Fig. 12; Table 1) in SAP2000 and comparing the values obtained by hand with those found in SAP2000 (Table 2).

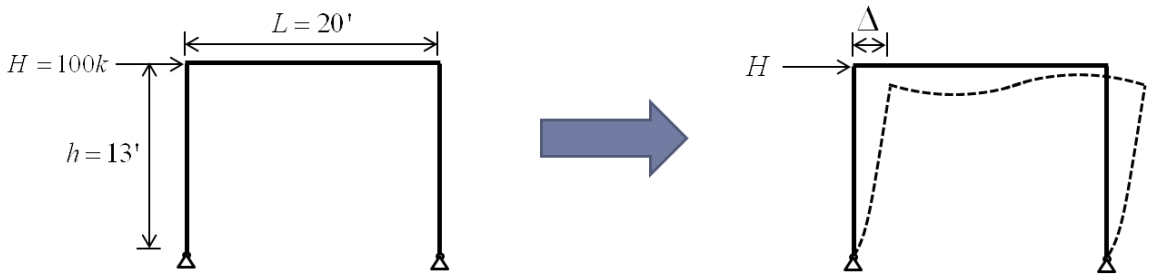

Fig. 12. Moment-resisting (portal) frame modeled in SAP2000 for comparison and deflected shape of frame

Table 1. Frame Properties

	Column	Girder
Cross-sectional area, A	2000 in^2	2000 in^2
Modulus of elasticity, E	29000 ksi	29000 ksi
Second moment of area, I	2000 in^4	200 in^4

Table 2. Frame Deflection

	Hand calc.	SAP2000 calc.
Horizontal deflection, Δ	9.483 in**	9.483 in

** $\Delta = H/k_{eq}$

Braced frames

Deflection equations

Consider the one-story, one-bay braced frame loaded as shown:

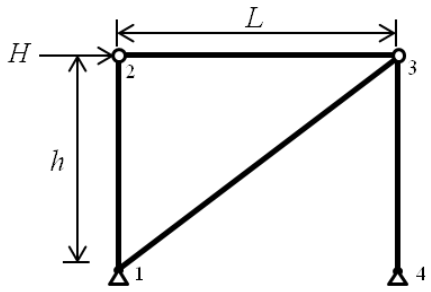

Fig. 13. Braced frame

Because every member frames into a pin at each end, neither shear force nor bending moment can act on the member itself. The internal axial forces in each member of the frame (Fig. 13) can be found by the Method of Joints (Table 3), with a positive sign denoting a tensile force and a negative sign denoting a compressive force.

Table 3. Internal Forces in Braced Frame

Member	Internal force (kips)
P_{12}	0
P_{13}	$H/L\sqrt{L^2+h^2}$
P_{23}	-H
P_{34}	-Hh/L

Since the left column (member 12) in the braced frame has force P_{12} equal to 0, that column can be considered a zero-force member. As such, its stiffness does not contribute to the system since it does nothing to resist the load.

Because each member in the braced frame can only support an axial load, the axial stiffness *k* can be obtained as follows:

$$\Delta = \frac{PL}{EA}$$
$$P = \frac{EA}{L}\Delta$$
$$\therefore\ k = \frac{EA}{L} \tag{10}$$

where Δ is the axial deformation of the member, P is the internal force in the member, L is the length of the member, E is the modulus of elasticity of the member, and A is the cross-sectional area of the member.

Much of the stiffness of the frame is due to the cross-bracing. This can be easily illustrated by imagining the braced frame from Figure 13 without any cross-bracing as shown below (Fig. 14):

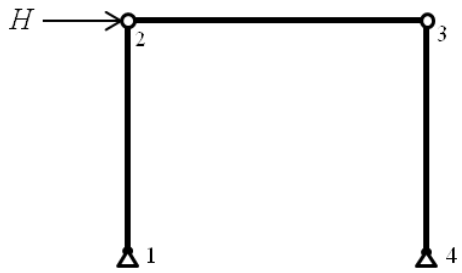

Fig. 14. Braced frame without cross-bracing

The frame in Figure 14 is essentially a truss with no cross-bracing. When the lateral load *H* is applied, the frame has no means by which to resist the load. Therefore, the frame will collapse immediately. The results in an equivalent stiffness value for the system of very nearly zero.

Because of the necessity of the bracing to the stability of the system, the stiffness k_B of the cross-brace is examined. The member 23 is allowed to deform under the applied load, while all other members are held rigid (i.e. undeformable). Equation (10) yields:

$$k_B = \frac{(EA)_B}{L_B} = \frac{(EA)_B}{\sqrt{L^2 + h^2}}$$

$$\Delta_B = \frac{F_B}{k_B} = \frac{\dfrac{H\sqrt{L^2 + h^2}}{L}}{\dfrac{(EA)_B}{\sqrt{L^2 + h^2}}} = \frac{H(L^2 + h^2)}{(EA)_B L}$$

where Δ_B is measured along the axis of the cross-brace.

Due to the geometry of the frame (Fig. 15),

$$\Delta = \frac{\Delta_B}{\cos\theta} \text{ where } \cos\theta = \frac{L}{\sqrt{L^2 + h^2}}$$

$$\therefore \Delta = \frac{H(L^2 + h^2)^{3/2}}{EAL^2}$$

where Δ depends solely on the deflection of the bracing because all other members are rigid.

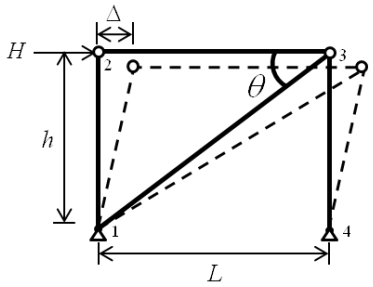

Fig. 15. Braced frame with θ defined

A similar analysis can be performed to determine the stiffness of the right-hand column (member 3,4 in Figure 15) and the deflection of the system due to the deflection of the column.

Equivalent stiffness

We can model the braced frame as an equivalent spring system with each spring in series with one another, as shown in Figure 16:

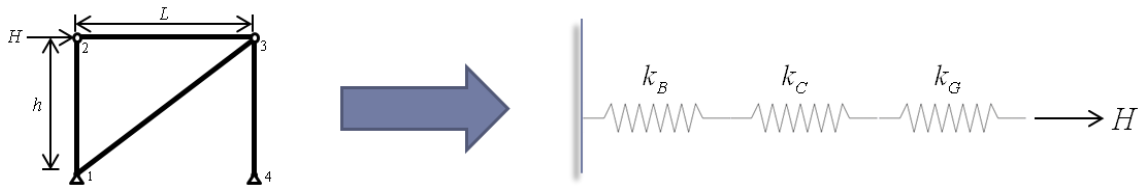

Fig. 16. Equivalent spring system for the left-hand side of braced frame

However, this model only provides the deflection for the left-hand side of the frame because each side of the frame deflects differently from the other due to the frame's asymmetry. The members in the equivalent system are in series with one another, so their equivalent stiffness can be obtained as follows:

$$\frac{1}{k_{eq}} = \frac{1}{k_B} + \frac{1}{k_C} + \frac{1}{k_G}$$

where k_{eq} is the equivalent stiffness of the system, k_B is the stiffness of the brace, k_C is the stiffness of the right-hand column, and k_G is the stiffness of the girder.

For the deflection of the right-hand side of the frame, the stiffness of the girder has no effect. The only two members whose deflections affect the deflection of the frame are the bracing and the right-hand column. The frame can be modeled as an equivalent spring system with each spring in series with one another, as shown in Figure 17:

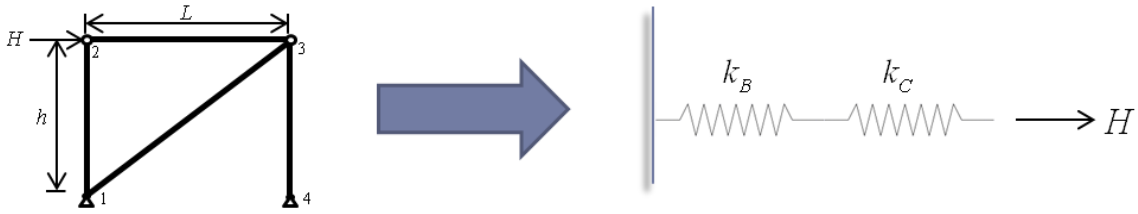

Fig. 17. Equivalent spring system for the right-hand side of braced frame

The members in the equivalent system are in series with one another, so their approximate stiffness can be obtained as follows:

$$\frac{1}{k_{eq}} = \frac{1}{k_B} + \frac{1}{k_C}$$

The braced frame shown in Figure 18 was created in SAP2000 to attempt corroborate the solutions found through solving the previously derived equations. The frame was made from steel with the area of the bracing equal to 5 in^2 and the areas of all other sections equal to 40 in^2. By varying the area of each member, its rigidity can be adjusted. The values produced by the SAP2000 analysis can be compared with those obtained by the previously derived equations in Table 4. (Note: Mass and the effects of gravity are neglected in this analysis.)

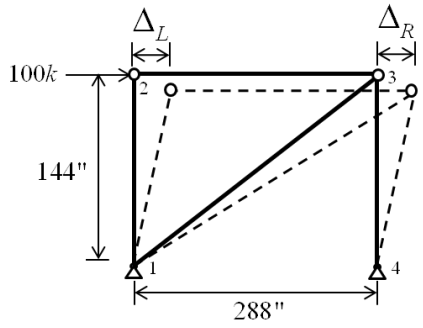

Fig. 18. Braced frame used in SAP2000 analysis and comparison

Table 4. SAP2000 Analysis Versus By-Hand Analysis

Flexible	Rigid	Δ_L in SAP	Δ_L by hand	Δ_R in SAP	Δ_R by hand
Brace	Columns, girder	0.2776 in	0.2776 in	0.2776 in	0.2776 in
Columns	Brace, girder	0.0031 in	0.0031 in	0.0031 in	0.0031 in
Girder	Brace, columns	0.0248 in	0.0248 in	0 in	0 in
All	---	0.3055 in	0.3055 in	0.2807 in	0.2807 in

CHAPTER V

EQUATION OF MOTION

To analytically model the motion induced into a single degree of freedom (SDOF) structure during a seismic event, a linear homogenous ordinary differential equation must be solved. The equation of motion for the SDOF system can be modeled as follows:

$$m\ddot{u} + c\dot{u} + ku = 0 \tag{11}$$

where *m* represents the mass of the system, *c* represents the damping coefficient, and *k* represents the stiffness of the system, while u, $\dot{u}$, and $\ddot{u}$ represent the relative displacement, velocity, and acceleration of the system measured from the supports.

The solution of equation (11) is of the form:

$$u(t) = Ce^{st} \tag{12}$$

Substituting equation (12) back into equation (11) and dividing by Ce^{st} yields the characteristic equation:

$$ms^2 + cs + k = 0 \tag{13}$$

Using the relationship:

$$\omega^2 = \frac{k}{m} \tag{14}$$

where ω is the natural frequency of the vibration, k is the spring constant (or structural stiffness), and m is the mass of the system, equation (14) can be substituted into equation (13) to achieve the following result:

$$s = -\frac{c}{2m} \pm \sqrt{\left(\frac{c}{2m}\right)^2 - \omega^2} \tag{15}$$

Due to the square root over the second term in equation (15), the second term varies among the following three cases over the course of the seismic loading depending on the damping coefficient c. The second term is:

- a real term if $c > 2m\omega$,
- a complex term if $c < 2m\omega$,
- or zero if $c_c = 2m\omega$, where c_c is referred to as the critical damping.

Thus, as the motion within the system persists, the damping always opposes the motion of the system. The damping gradually dissipates the energy initially input into the system, therefore causing the motion to decrease with increasing time (Boyce and DiPrima 2011; Chen and Scawthorn 2003; Chopra 1981).

CHAPTER VI

METHODS

This research focuses on the usage of passive friction damping in braced frames exposed to seismic vibrations. Experimentation is performed on scale models of a single-story, single-bay braced frame. The models used for this experimentation are designed to facilitate comparison of the displacements and accelerations between a case *without* damping and a case *with* damping. The virtual models are analyzed in SAP2000 using nonlinear dynamic time-history analysis. The results of these models are then corroborated by experimentation performed on a physical model of the scale building. Free vibration tests are performed on the model, and then the model is tested on a shake table for final validation.

The dynamic behavior of each building is classified by its peak acceleration at the first floor, which is directly proportional to the peak displacement of the frame and thus to the damage due to the seismic energy input. Although this measure does not describe the effect of the earthquake on the structure in its totality, the acceleration time histories can be used as indicators of the structure's dynamic behavior and of the effectiveness of the device under investigation.

Virtual modeling

Two models are created in SAP2000 for analysis, a scale model of a one-story building (Figs. 19 and 20) without additional damping modeling the effect of the friction device and a scale model of the same building with the additional damping included. Because of the symmetry of the scale model, it can be modeled as a two-dimensional frame to lower the computation effort required to perform the analysis. Therefore, the scale model considers the building to be 8.5 inches tall with a length measuring 12 inches in the plane of motion. Motion is induced in the plane of the cross-bracing (Fig. 19), while the framing in the other planes serves merely to stabilize the model and is therefore omitted from the SAP2000 model (Fig. 20). The members are modeled as brass tubing (with material properties listed in Table 5).

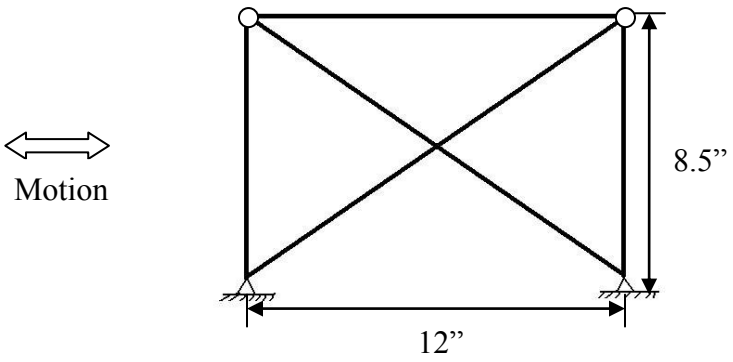

Fig. 19. View of cross-braced frame in the plane of motion

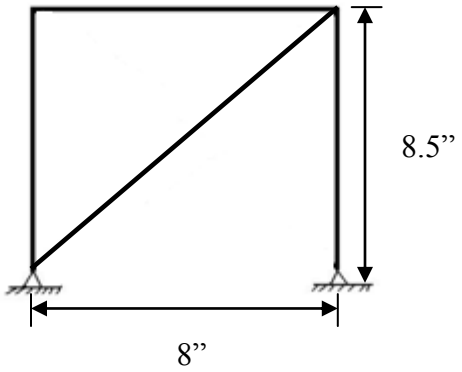

Fig. 20. View of cross-braced frame out of the plane of motion

Table 5. Brass Material Properties

Weight per unit volume	2.950E-04 kips/in^3
Modulus of elasticity, E	15300 ksi
Poisson’s ratio, U	0.33
Coefficient of thermal expansion, A	12.40 μin/in-°F
Shear modulus, G	5750 ksi

The main frame (i.e. the columns, the girders, and the out-of-plane bracing) comprises brass piping with an outside diameter of 0.1250 inches and an inside diameter of 0.0780 inches. The in-plane cross-bracing comprises two types of brass piping with one fitting inside the other. The outer pipe has an outside diameter of 0.1645 inches and an inside diameter of 0.1115 inches, while the dimensions of the inner pipe depend on whether it models a friction damping device. The pipe that models a brace *without* a friction damper installed has outside diameter of 0.0950 inches and an inside diameter of 0.0490 inches. The difference between the inner diameter of the larger pipe and the outer diameter of the smaller pipe results in a negligible friction coefficient. The pipe that

models a brace *with* a friction damper installed has an outside diameter of 0.1250 inches and an inside diameter of 0.0780 inches. In this case, the inner diameter of the larger pipe is smaller than the outer diameter of the smaller pipe, resulting in a measureable friction coefficient. This resulting friction between the pipes models the effect of friction damping on the structure as it undergoes an excitation. These dimensions are summarized in Table 6.

Table 6. Scale Model Member Dimensions

	Main frame	Outer pipe	Inner pipe without friction	Inner pipe with friction
Outer diameter	0.1250 inches	0.1645 inches	**0.0950 inches**	**0.1250 inches**
Inner diameter	0.0780 inches	**0.1115 inches**	0.0490 inches	0.0780 inches

The joints at the base of each model are considered to be pinned, and the major (M_{22}) moments at the joints B and C (Fig. 21) are released to approximate pinned connections. The 1-kilogram mass supported by the structure along member BC is not applied directly to the structure as a concentrated load in SAP2000; it is instead considered as a distributed load along the top of the first floor. The p-delta effect is also taken into account to ensure more accurate results using the settings provided for the dynamic analysis in SAP2000. Rayleigh damping is accounted for, the parameters of which are determined via free vibration testing. The mode 1 period of the frame is 0.3701 seconds and the mode 2 period is 3.795E-04 seconds.

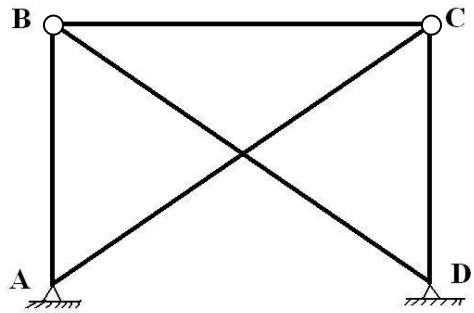

Fig. 21. Side view of cross-braced frame used in modeling with joint labels

Compared to the stiffness of the spring located at the center of the cross brace, the stiffnesses of the columns and girders are significantly higher. To model this in SAP2000, either the area of these members or their moduli of elasticity should be treated as significantly larger than that of the brace. Therefore, to achieve this distinction, the moduli of elasticity of the columns and girders are arbitrarily made significantly larger.

The effect of the friction in the friction device is modeled in SAP2000 using equivalent viscous damping, which is estimated from the results of free vibration tests using equation (17):

$$\zeta = \frac{1}{2\pi j} \ln\left(\frac{\ddot{u}_i}{\ddot{u}_{i+j}}\right) \tag{17}$$

In the frame with no friction device installed, inherent damping exists, despite the lack of an overtly added friction device and ζ equals 0.1029. In the frame modeling the friction device, ζ equals 0.1936. This viscous damping is then modeled in SAP2000 by inserting into the cross brace a spring element with an elastic spring constant (or brace

stiffness) *k* approximated as 2.475E-03 k/in, a post-yield stiffness ratio *r* of 1E-03, a yield strength of 0.1, and a yielding exponent *exp* of 10 (Peternell 2009).

The two-dimensional representation of the braced frame in SAP2000 (Fig. 22) is analyzed to obtain the final results. Note the moment releases at the top two nodes, the pinned connections at the bottom two nodes, and the spring element forming the cross brace. Additionally note that the second cross-brace is not included in the SAP2000 model since the spring element is defined so that it will not buckle in compression, thus rendering the second cross-brace redundant.

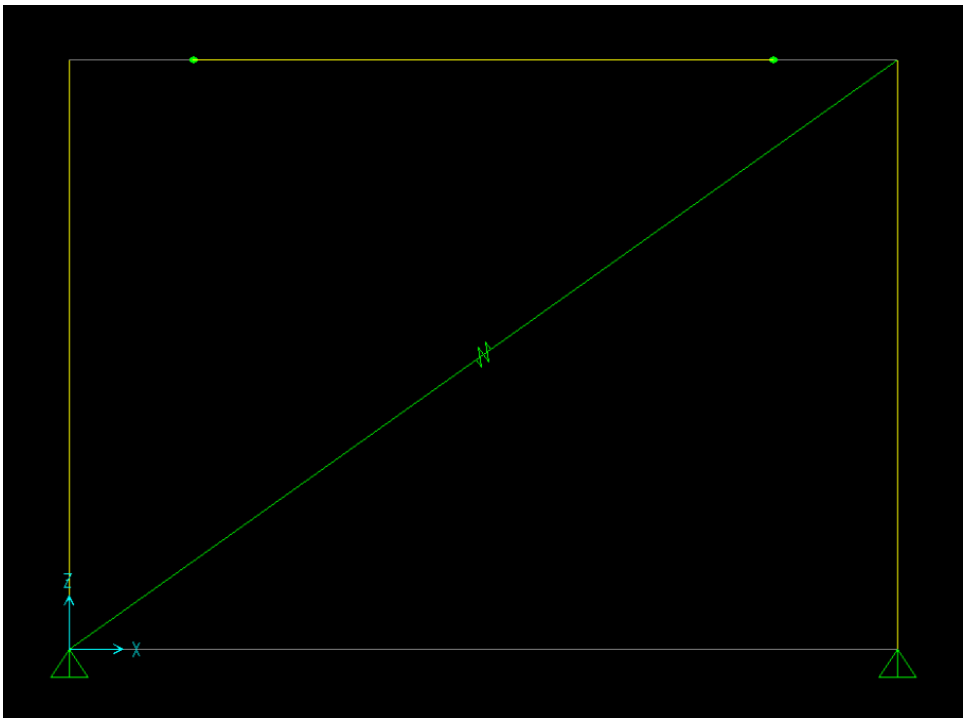

Fig. 22. SAP2000 model of cross-braced frame

Physical modeling

To ensure that the results yielded by SAP2000 are accurate, follow-up analysis is performed on a physical model. To create the physical scale model, brass tubing (Table 5) is used to form the cross-braced frame (Fig. 19 and 20), while a ¼" x 4" x 12" piece of wood forms the in-plane girder. Each connection in the plane of motion is formed with a hinge to approximate a pinned connection. The nodes at the ground level are affixed to the top of the shake table with hinges also so that their moments are released. The cross-braces (without friction damping) are created by sliding the smallest brass pipe within the largest brass pipe (Table 6) then soldering a small spring at the location of the intersection. The spring is installed between these two pipes to return the model to its original shape after each excitation, ensuring the structural stability of the system. The difference between the inner diameter of the largest pipe and the outer diameter of the smallest pipe is enough that the friction resulting from their interaction as the model undergoes an excitation is negligible.

The friction devices are created along each cross brace by affixing a second length of bracing parallel to the original approximately frictionless bracing. A midsize brass tube is fit within the largest diameter brass tube (Table 6). In this case, the inner diameter of the larger pipe is smaller than the outer diameter of the smaller pipe, resulting in a measureable friction coefficient. Finally, a 1-kilogram mass is affixed to the wood that forms the first floor of the structure.

The shake table is programmed to induce vibrations according to the recorded ground motion of the 1995 Kōbe Earthquake (Peternell 2009). Accelerometers are attached to the model to provide digital readings of the accelerations at both the ground level and the first story and to monitor the effects of the accelerations on the structure. An encoder is affixed to the shake table to record data corresponding to the ground displacement. The physical model is shown in Figure 23 in its entirety. Figures 24 through 27 provide more focused views of various aspects of the model.

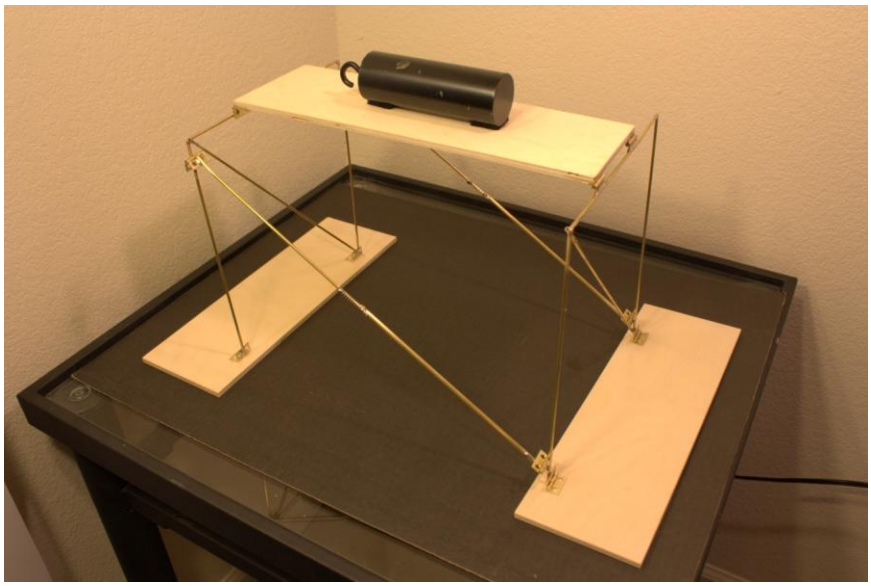

Fig. 23. Orthographic view of the physical model

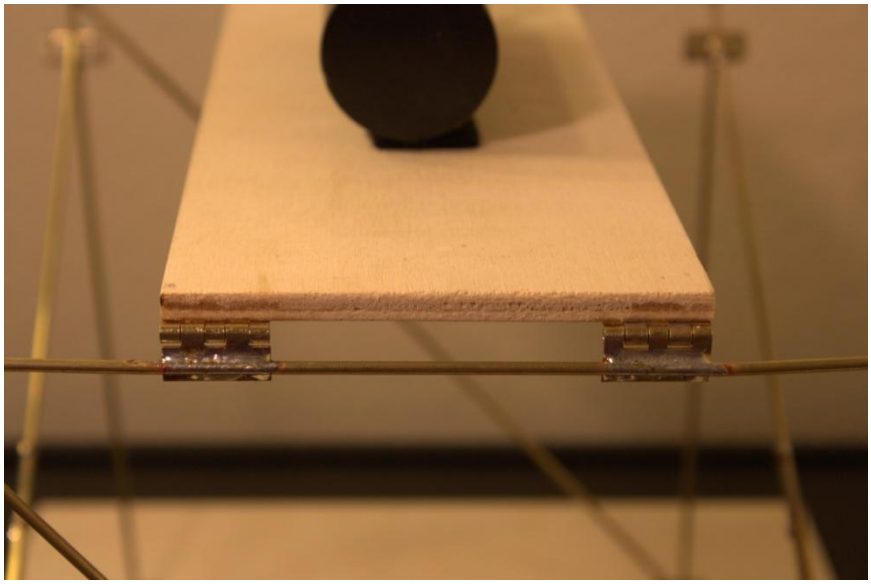

Fig. 24. Out-of-plane view focused on girder connections

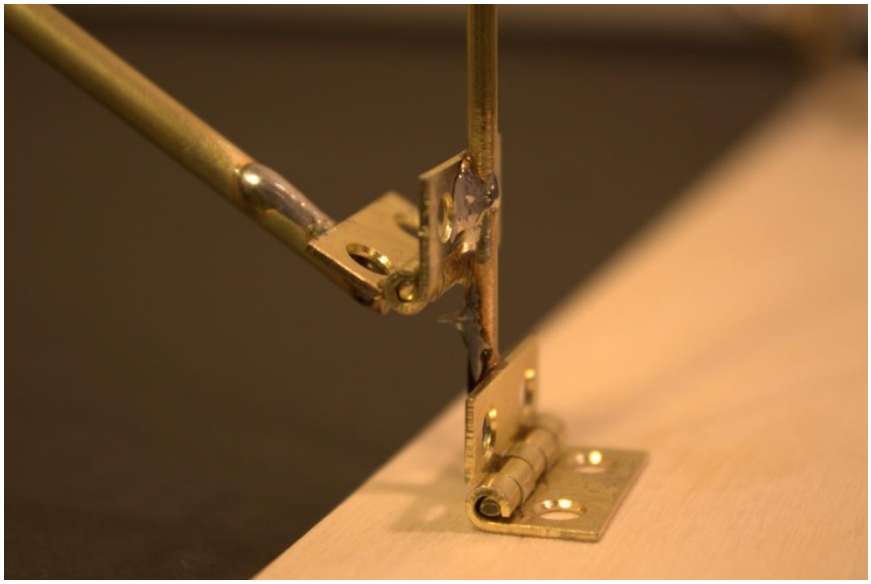

Fig. 25. Hinges connecting cross-brace to column and column to floor

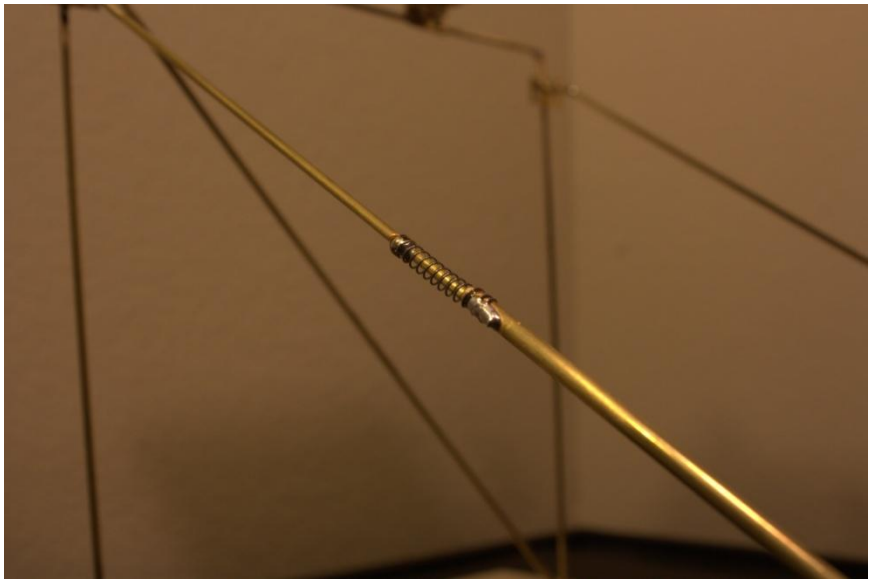

Fig. 26. Foreground: in-plane bracing with spring element and without friction damper
Background: out-of-plane bracing

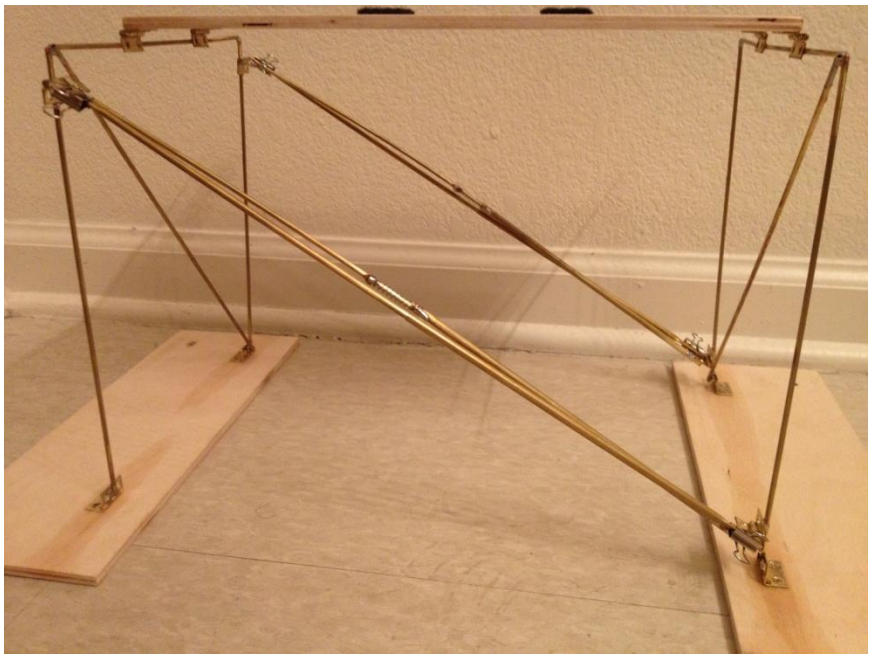

Fig. 27. Physical model with friction damper attached

Fig. 28. In-plane bracing with spring element and friction damper

CHAPTER VII

RESULTS

As was detailed in Chapter VI, virtual modeling was performed in SAP2000, and a physical model was tested to corroborate these results. Both the SAP2000 model and the physical model were exposed to the ground motion recording of the 1995 Kōbe Earthquake (Fig. 29).

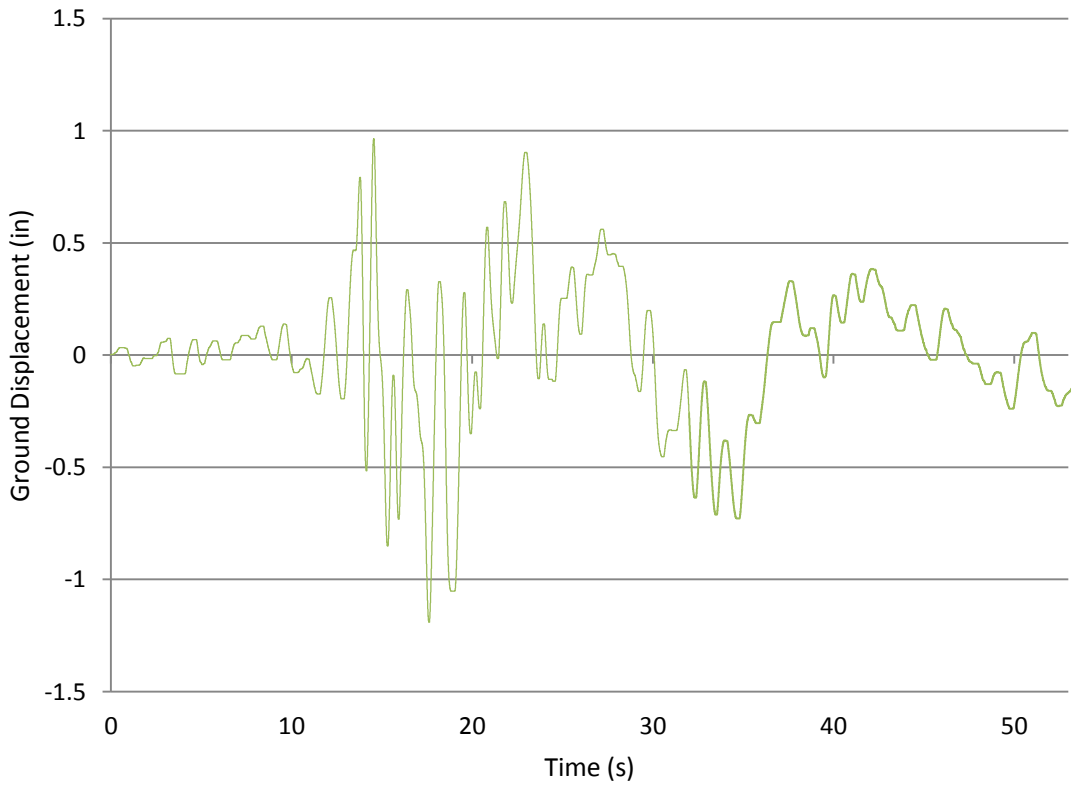

Fig. 29. Ground motion recording of the 1995 Kōbe Earthquake

The following graphs (Figs. 30 and 31) plot the acceleration of the first floor of the physical model as a function of time as the model experiences the ground motion recording shown in Figure 29.

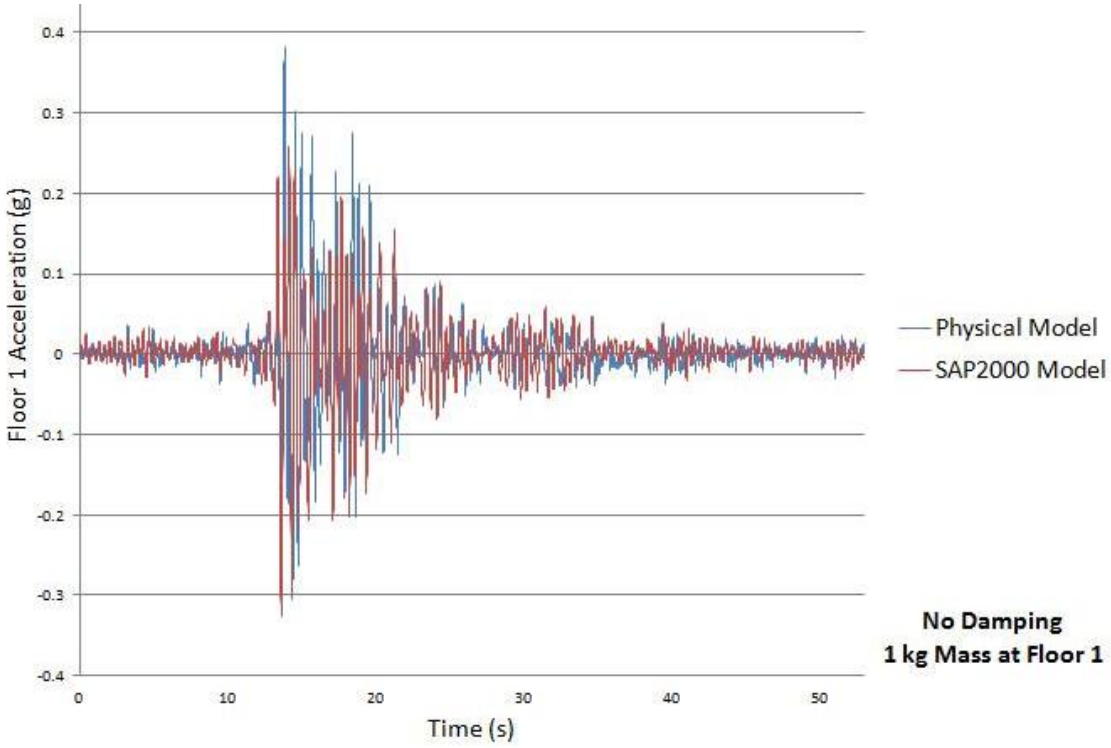

Fig. 29. First floor acceleration versus time without friction damping

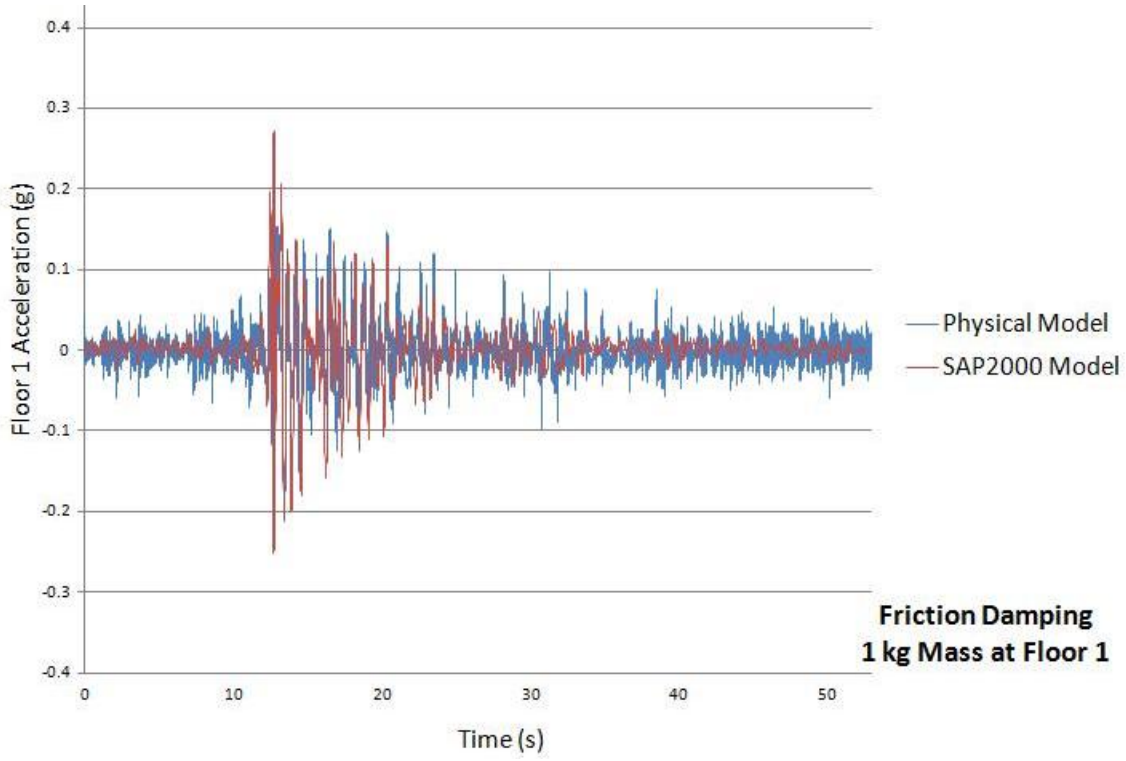

Fig. 31. First floor acceleration versus time with friction damping

The blue plot in Figures 30 and 31 represents the time history of the accelerations experienced by the first floor of the model. The red plot in the figures represents the time history of the accelerations that SAP2000 calculated were experienced by the first floor of the model. While these data do not provide a perfect match, the distinct similarities provide a good basis for validation of the data. The friction damping device reduced the peak excitation by more than 50% in the physical model (blue plot) between Figures 30 and 31. The friction damping also reduced the overall peak excitation between the two models from 0.4 g to 0.3 g, which represents a fairly significant reduction given the scale.

CHAPTER VIII

CONCLUSIONS

During an earthquake, a large amount of seismic energy is input into the structures built on the Earth's surface. This energy results in vibrations that can cause significant damage to the structure, leading to lowered structural integrity and even to collapse. Due to the inevitability of seismic activity, incorporating devices to control the motion induced by seismic vibrations is crucial to reducing the structural, social, and financial damage caused by earthquakes.

To diminish the amount of seismic energy input into the members of a structure, numerous devices have been developed to control these vibrations. In recent years, the development of technology suited to active (and hybrid) seismic vibration control has advanced. With this, many researchers have shifted their focuses to active and hybrid systems, slowing the development of passive systems due to the lack of attention paid to the subject. However, passive systems have many desirable features. They are incredibly simple, easy to retrofit, and highly effective.

This study investigated the performance of passive friction damping as employed in friction-damped braced buildings. It sought to examine an analytical model of a structure both with and without effective friction damping then to achieve similar results through

physical experimentation on a shake table. The experimental results verified the results obtained by the analytical model, as hypothesized.

Both the analytical and the physical models were exposed to the ground motion recording of the 1995 Kōbe Earthquake. The acceleration of the first floor of the physical model as a function of time was compared to that of the analytical model. In this analysis, the friction damping device reduced the peak acceleration by 50% in the physical model. The friction damper also reduced the overall peak acceleration between the models by 25%.

Reducing the magnitude of the acceleration transmitted to the structure results in a reduction of the force input into the structure by the mass due to Newton's second law, represented as $F = ma$. A reduction of acceleration by 50% results in a 50% reduction of force transmitted into the structure by the mass.

Further experimentation to determine the most effective friction coefficient to be utilized within the friction damper may provide interesting insight into the dynamic behavior of friction-damped braced frames. Another potential route of exploration might be to incorporate other types of passive damping (e.g. base isolation, fluid damping, etc.) into a structure with passive friction damping and to quantify the benefits of these combinations when the structure is exposed to a seismic loading.

The validation of the virtual models by the physical model provides credence to the usage of friction-damped braced frames as a seismic energy dissipating system. With wider implementation of these devices, safer environments can be expected in seismically-active areas.

REFERENCES

Boyce, W. E., and DiPrima, R.C. (2011). *Elementary differential equations*, John Wiley & Sons, Hoboken, NJ, 137-218.

Chen, W-F., and Scawthorn, C. (2003). *Earthquake engineering handbook*, CRC Press, Boca Raton, FL.

Chopra, A. K. (1981). *Dynamics of structures: a primer*, Earthquake Engineering Research Institute, Berkeley, CA.

Elnashai, A. S., and Di Sarno, L. (2008). *Fundamentals of earthquake engineering*, John Wiley & Sons, Chichester, United Kingdom.

Encyclopædia Britannica Inc. (2012). "Kōbe earthquake of 1995." *Encyclopædia Britannica Online*, < http://www.britannica.com/EBchecked/topic/873249/Kobe-earthquake-of-1995> (Apr. 1, 2012).

Gamesby, R. (2012). "The Kobe Earthquake – an earthquake affecting an MEDC." *Cool Geography*, < http://www.coolgeography.co.uk/GCSE/Year11/Managing%20 Hazards/Earthquakes/kobe.htm> (Mar. 19, 2012).

Hu, Y-X., Liu, S-C., and Dong, W. (1996). *Earthquake engineering*, E & FN Spon, London.

Keightley, W. (1977). "Building damping by Coulomb friction." *Proc., 6th WCEE*, New Delhi, India, 3043-3048.

Keightley, W. (1979). *Prestressed walls for damping earthquake motions in buildings*, Montana State University, Dept. of Civil Engineering and Mechanics.

Mead, D. (1998). *Passive vibration control*, John Wiley & Sons, Chichester, England.

Pall, A., and Marsh, C. (1982). "Seismic response of friction damped braced frames." *Journal of the Structural Division*, 108(6), 1313-1323.

Pall, A., Marsh, C., and Fazio, P. (1980). "Friction joints for seismic control of large panel structures." *Journal of Prestressed Concrete Institute*, 25(6), 38-61.

Pall, A., and Pall, R. T. (2004). "Performance-based design using Pall friction dampers - An economical design solution." *Proc., 13th World Conference on Earthquake Engineering*, Vancouver, B. C., Canada.

Peternell, L. E. A. (2009). "Seismic interstory drift demands in steel friction damped braced buildings," thesis, presented to Texas A&M University, at College Station, TX, in partial fulfillment of the requirements for the degree of Master of Science.

Somerville, P. G., Smith, N. F., Punyamurthula, S., and Sun, J. I. (1997). "Development of ground motion time-histories for phase 2 of the FEMA/SAC steel project." *Rep. No. SAC/BD-97/04*, SAC Joint Venture, Sacramento, CA.

Soong, T. T., and Constantinou, M. C., eds. (1994). *Passive and active structural vibration control in civil engineering*, CISM Courses and Lectures, Springer, New York.

Soong, T. T., and Dargush, G. F. (1997). *Passive energy dissipation systems in structural engineering*, Wiley, New York.

Soong, T. T., and Spencer, B. F. (2002). "Supplementary energy dissipation: State-of-the-art and state-of-the-practice." *Eng. Struct*., 24, 243-259.

Villaverde, R. (2009). *Fundamental concepts of earthquake engineering*, CRC Press, Boca Raton, FL.

CONTACT INFORMATION

Name:	Brynnan Elyse Fink
Professional Address:	c/o Dr. Gary T. Fry Department of Civil Engineering Texas A&M University 3136 TAMU College Station, TX 77843
Email Address:	befink92@tamu.edu
Education:	B.S., Civil Engineering, Texas A&M University, May 2013 Summa Cum Laude Honors Undergraduate Research Fellow Chi Epsilon Phi Kappa Phi Tau Beta Pi